Severe Infantile Encephalomyopathy Caused by a Mutation in COX6B1, a Nucleus-Encoded Subunit of Cytochrome C Oxidase

Valeria Massa,[1,7] Erika Fernandez-Vizarra,[1,7] Saad Alshahwan,[2] Eman Bakhsh,[3] Paola Goffrini,[4] Ileana Ferrero,[4] Paolo Mereghetti,[5] Pio D'Adamo,[6] Paolo Gasparini,[6] and Massimo Zeviani[1,*]

Cytochrome c oxidase (COX) deficiency, one of the most common respiratory-chain defects in humans, has been associated with mutations in either mitochondrial DNA genes or nucleus-encoded proteins that are not part in but promote the biogenesis of COX. Mutations of nucleus-encoded structural subunits were sought for but never found in COX-defective patients, leading to the conjecture that they may be incompatible with extra-uterine survival. We report a disease-associated mutation in one such subunit, COX6B1. Nuclear-encoded COX genes should be reconsidered and included in the diagnostic mutational screening of human disorders related to COX deficiency.

Introduction

Cytochrome c oxidase (COX, complex IV), the terminal enzyme in the mitochondrial respiratory chain, catalyzes the electron transfer from reduced cytochrome c to molecular oxygen. This reaction is coupled to the extrusion of protons from the mitochondrial matrix to the intermembrane space, forming a proton-based membrane potential that allows ATP to be synthesized. In mammals, the COX monomer is composed of 13 subunits, but the active form of the enzyme works as a dimer in vivo. Mitochondrial DNA (mtDNA) encodes the three larger, and most hydrophobic, subunits, including the two catalytic MT-CO1 and MT-CO2 subunits, as well as the core structural MT-CO3 subunit. The remaining ten smaller subunits, COX4, 5A, B, 6A, B, C, 7A, B, C, and 8, some of which have also tissue-specific isoforms, are encoded in the nucleus and imported into mitochondria.[1] Most of the nuclear encoded subunits of COX have hydrophobic domains spanning the inner mitochondrial membrane once.[2] However, subunits COX5A, COX5B, and COX6B are hydrophilic extramembrane proteins, the first two facing the matrix, whereas COX6B faces the intermembrane space. According to the bovine enzyme structure, COX subunit 6B, a 10 kDa polypeptide, connects the two COX monomers into the physiological dimeric form[2,3] and is also believed to interact with cytochrome c.[4,5]

COX deficiency (MIM 220110) is one of the most common respiratory-chain defects in humans, being associated with different clinical phenotypes and caused by different genetic abnormalities. The study of COX defects is complicated as the biosynthesis and function of the enzyme depends on the contribution of both mitochondrial and nuclear encoded products.

Mutations in mtDNA-encoded COX genes (MIM 516030, 516040, and 516050) are associated with a range of phenotypes including pure myopathy, MELAS (MIM 540000), encephalomyopathy, and a motor neuron disease-like presentation.[6] In other cases, COX deficiency is associated with mutations in nuclear-encoded proteins that do not belong to, but participate in the biogenesis of, complex IV.[7] Mutations in nuclear-encoded COX structural subunits were searched for but never found.[8–11]

We studied two siblings belonging to a consanguineous Arab family originating from the Saudi-Yemeni border, presenting with a combination of early-onset leukodystrophic encephalopathy (Figures 1A and 1B), myopathy, and growth retardation associated with COX deficiency of unknown cause. Linkage analysis followed by sequencing of candidate genes revealed the presence of a missense mutation in the *COX6B1* gene.

Subjects and Methods

Subjects

Written informed consent was obtained by the parents of the patients and investigations were carried out according to the guidelines of the Ethical Committee of the "Fondazione Istituto Neurologico Carlo Besta," in agreement with the Italian and European Union law.

The patients, both affected by similar leukodystrophic changes (Figures 1A and 1B), were the two youngest brothers of a family composed of five sibs from third-degree cousin parents of Saudi Arabian origin (Figure 2A). A sister and brother of the patients are alive and well. A fifth female child died immediately after birth because of ventilation difficulty. The mother had previously had a second trimester miscarriage. The first patient (individual AK, #15 in

[1]Department of Molecular Neurogenetics, Foundation IRCCS Neurological Institute "C. Besta," 20126 Milano, Italy; [2]Department of Pediatrics, [3]Department of Neuroradiology, Riyadh Military Hospital, 11159 Riyadh, Saudi Arabia; [4]Department of Genetics Anthropology Evolution, University of Parma, 43100 Parma, Italy; [5]Department of Biotechnology and Biosciences, University of Milano-Bicocca, 20126 Milano, Italy; [6]Department of Medical Genetics, IRCCS Burlo Garofolo-University of Trieste, 34137 Trieste, Italy
[7]These authors contributed equally to this work
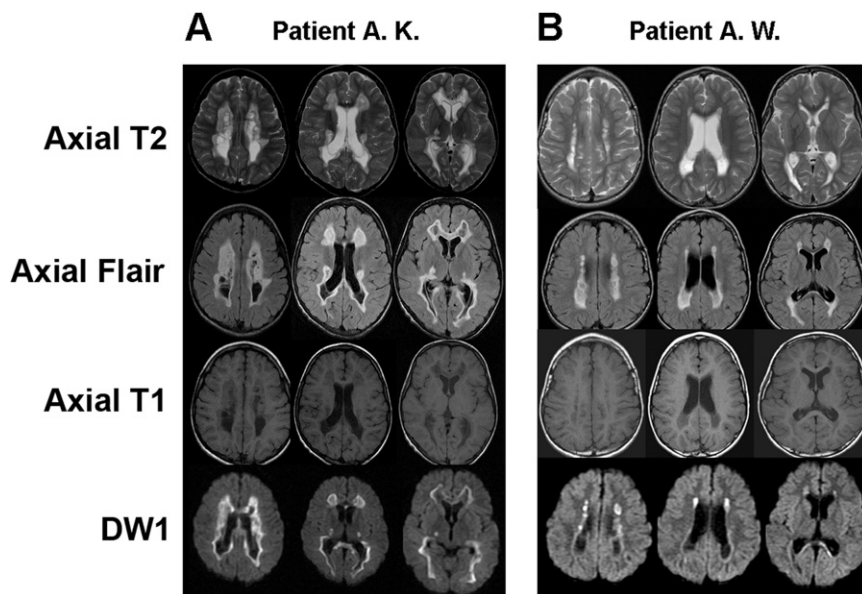*Correspondence: zeviani@istituto-besta.it

Figure 1. Brain MRI Panel
(A) Patient AK at 9 years of age. Bilateral, symmetrical signal abnormalities affect the frontal, parietal, and occipital white matter, as well as the splenium and the genu of the corpus callosum. Numerous cystic lesions are also present, particularly in the anterior periventricular regions, with ex vacuo dilation of the lateral ventricles. (B) Patient AW at 6 years of age presented symmetrical white matter hyperintensity in the periventricular region, with cystic vacuolation. The splenium of the corpus callosum is also involved.

Methods
Linkage Analysis
Genome-wide search was performed with the ABI PRISM Linkage Mapping Set v.2.5 (ABI), characterized by over 375 markers that define a 10 cM resolution human index map. Polymerase chain reactions (PCRs) with fluorescently labeled primers were run under the conditions suggested by the supplier. An aliquot of each PCR was run on an ABI PRISM 3130 DNA sequencer, and results were processed by GENEMAPPER software. Statistical analysis was performed on the basis of an autosomal-recessive disease with complete penetrance. The disease-gene frequency was set to 0.001, and all marker alleles were considered to be equally frequent. Haplotyping and multipoint parametric analysis were performed by SimWalk2[12–14] v.2.91 with Markov chain Monte-Carlo (MCMC) and simulated annealing algorithms. Files for SimWalk analysis were prepared with the Mega2[15] software version 3.0.

Sequence Analysis
Molecular analysis was performed on genomic DNA extracted either from muscle or fibroblasts. Overlapping PCR-amplified fragments of the four *COX6B1* exons were sequenced in a 3100 ABI Prism Automated Sequencer. The presence of the mutated allele in patients and controls was also assessed by restriction fragment length polymorphism (RFLP) with the restriction enzyme Fnu4HI and denaturing high-performance liquid chromatography (DHPLC) analysis of PCR products.

Protein Modeling
Protein modeling was carried out on the crystal structure of bovine COX in fully reduced state (PDB code 2EIJ). The ionic interactions of the R19 residue were identified with the online software Protein Interaction Calculator.

Cell Culture and Media
Cells were cultured in Dulbecco's modified Eagle's medium (DMEM) supplied with 10% fetal calf serum at 37°C in a 5% CO2 atmosphere. Fibroblasts from both patients and control were immortalized by electroporation of the cells with the pBABE40 plasmid and subsequent selection with 0.5 μg/ml puromycin in the culture medium.[16]

The full-length human IMAGE complementary DNA (cDNA) clone for *Homo sapiens COX6B1* (accession number BC002478) was obtained from the RZPD (clone IRAUp969D1010D6) and was used to generate the cDNA fragment by amplification. The PCR products were cloned into the pcDNA3.2/V5/GW/D-TOPO vector (Invitrogen). The G→A substitution found in the patients

Figure 2A) was the product of uneventful pregnancy. Birth weight and height are not known but were reported as abnormally low and remained below the 3rd percentile ever since. He was a thin boy, with reduced muscle mass, but the psychomotor milestones were reached timely and appropriately. At 6 years he was admitted for the first time to the Riyadh Military Hospital because of muscle weakness and pain. During a subsequent hospitalization at 10 years he was found to suffer of muscle weakness, cognitive deterioration, and visual loss. The visual evoked potentials were absent, whereas the brainstem potentials were present and normal. The lower cervical and upper cervical somatosensory evoked potentials were reduced in amplitude. An electromyography (EMG) showed signs of lower and upper motor neuron involvement. An electroencephalogram (EEG) showed a poorly organized, slow background rhythm with no photic reaction and no epileptic discharges. Several brain magnetic resonance imaging (MRI) examinations showed progressive, diffuse leukodystrophic changes in the cerebellum, pyramidal tracts and supratentorial white matter, with later development of white matter vacuolation from the peritrigonal toward the frontal areas, and ex vacuo dilatation of the lateral ventricles (Figure 1A). The patient died at 10 years by rapidly progressive neurological deterioration after recurrent generalized convulsions and severe metabolic acidosis with very high serum lactic acid levels. The second patient (individual AW, #16 in Figure 2A) had a clinical course similar to, but milder than, that of the elder brother. He was born after uneventful pregnancy; birth weight was 2.6 Kg, head circumference was 33 cm, and height was 47 cm. He was kept in the nursery because of poor sucking and difficulty in breathing. The psychomotor development was normal until 6 years of age, when he experienced repeated episodes of unsteady gait and visual disturbances. Presently he is an 8-year-old boy with mild trunk and limb ataxia, muscle weakness, reduced visual acuity, and moderate cognitive deterioration (IQ = 84). The body weight is 19 Kg (90th centile), height is 110 cm (3rd centile). Laboratory investigation showed high serum lactate levels (2.6 mM, normal value [n.v.] < 1.8) and cerebrospinal fluid (CSF) (5.1 mM, n.v. < 1.8). EMG showed predominantly myopathic changes; gas chromatography-mass spectrometry (GC-MS) analysis of urine was normal. Brain MRI showed symmetrical, diffuse leukodystrophy with cystic lesions in the supratentorial areas of the white matter (Figure 1B).

was introduced in the recombinant cDNA by site-directed mutagenesis with the Quick Change Kit (Stratagene). The recombinant plasmids encoding the wild-type and mutated *COX6B1* cDNAs were transfected by electroporation into the immortalized fibroblast cell lines and underwent antibiotic selection by addition of G418 (200 μg/ml) to the culture medium to create the stably transfected cell lines.

Biochemical Analysis

Biochemical activity assays of the individual respiratory-chain complexes in cultured primary and immortalized skin fibroblasts lysates obtained by treatment with digitonin and in muscle homogenate were carried out according to.[17] Specifically, measurements of cytochrome c oxidase activity were performed spectrophotometrically after the decrease of absorbance at 550 nm, because of oxidation of cytochrome c, during 120 s at 38°C.[18] The same experiments were carried out in yeast-isolated mitochondria at 30°C. Enzymatic activity of each complex was normalized to that of citrate synthase.

Analysis of COX Assembly

Mitochondrial fractions were isolated from immortalized fibroblasts and HeLa cells as previously described,[19] lysed, and then electrophoresed through a sodium dodecyl sulfate (SDS)-Urea-Glycerol denaturing polyacrylamide gel.[20] For the detection of the assembled complex IV in control and patient skin fibroblast and muscle biopsies, blue-native gel electrophoresis (BNGE) was used. Samples were obtained from 2×10^6 cultured fibroblasts or 25 mg of muscle biopsy,[21] or through the use of isolated mitochondria from 15×10^6 cultured cells,[22] with slight modifications. Twenty microliters of sample were loaded and run into a 5%–13% gradient nondenaturating first dimension (1D)-BNGE. For western blot (WB) analysis, the gels were electroblotted onto polyvinylidene difluoride (PVDF) filters and sequentially immunostained with specific antibodies against different COX subunits and the 30 kDa subunit of complex II (SDH) for normalization purposes. All the antibodies used were commercial and supplied by Molecular Probes (Invitrogen).

Analysis of Yeast Models

Yeast strains used were BY4741 (MAT**a**; *his3Δ1 leu2Δ0 lys2Δ0 ura3Δ0*) and its isogenic *cox12::kanMX4* mutant (Euroscarf collection). Cells were cultured in yeast nitrogen base (YNB) medium (0.67% yeast nitrogen base without amino acids [Difco]) supplemented with 1 g/l of drop-out powder containing all amino acids except those required for plasmid maintenance. Various carbon sources were added at 2% (w/v). Media were solidified with 20 g/l agar. For respiration analysis, cells were grown to late-log phase in the YNB medium supplemented with 0.5% glucose.

Transformation of yeast strains was obtained by the lithium acetate method.[23] Restriction-enzyme digestions, *Escherichia coli* transformation, and plasmid extractions were performed with standard methods.[24] Oxygen uptake rate was measured at 30°C with a Clark electrode in a reaction vessel of 3 ml of air-saturated respiration buffer (0.1M phthalate–NaOH [pH 5.0]), 10 mM glucose, starting the reaction with the addition of 20 mg of wet weight of cells as previously described.[25]

The *S. cerevisiae* expression vector pYEX-BX (Clontech) was employed. The wild-type human *COX6B1* cDNA was cloned in EcoRI-digested pYEX plasmid under the control of *CUP1* promoter. The point mutation corresponding to that found in the patient was generated with the QuickChange Site Directed Mutagenesis kit from Stratagene.

RNA Interference and mRNA Analysis and Quantification

The small interfering RNA (siRNA) candidate targets, used to design the short hairpin RNA (shRNA) oligonucleotides to be cloned into the expression vectors, aiming at different positions in the 5′ untranslated region (UTR) and 3′ UTR of the *COX6B1* messenger RNA (mRNA), were calculated with a web-based algorithm. The oligonucleotide pairs were cloned into pSuper.gfp/neo and pSuperior.puro expression vectors (OligoEngine) according to the manufacturer's instructions. HeLa cells were transiently transfected by electroporation with the four different constructs cloned into pSuper.gfp/neo, allowing the evaluation of the transfection efficiency by fluorescence detection of the enhanced green fluorescent protein (EGFP) expression. The amount of the *COX6B1* mRNA, quantified 72 hr after transfection, showed that the constructs expressing the shRNAs corresponding to sequences 1 (COX6B1sh1) and 14 (COX6B1sh14) were the most efficient in knocking down the expression of the *COX6B1* transcript. HeLa cells stably expressing COX6B1sh1 or COX6B1sh14 were obtained by transfection of the constructs in pSuperior.puro vector and selection of cells by the addition of puromycin (0.25 μg/ml) to the culture medium. RNA from cultured cells was extracted with the RNeasy mini kit (QIAGEN). Then, the RNA was retrotranscribed by random primers in the Cloned AMV First-Strand cDNA Synthesis Kit (Invitrogen). The amount of *COX6B1* mRNA was quantified by real-time PCR with the Power SYBR Green PCR Master Mix (Applied Biosystems).

Statistical Analysis

Differences in COX activity between the different cell lines was assessed with the unpaired, two-tail Student's t test. The tests and calculations were performed with the Statview 5.0 software.

Results

Morphological and Biochemical Studies

The histochemical reaction to COX was diffusely low in a skeletal muscle biopsy from patient AK (Figure 2B). The COX specific activity normalized to that of Citrate Synthase (CS, and index of mitochondrial mass, was drastically reduced in muscle homogenates from both patients (approximately 20% of the normal mean), and it was mildly but significantly reduced also in primary and immortalized cultured fibroblasts (approximately 50% from both patients); the activities of other respiratory complexes were normal in both tissues (Tables 1 and 2).

Linkage Analysis and Mutation Screening

Genome-wide linkage analysis allowed us to identify a unique locus of continuous homozygosity between recombinant DNA microsatellite markers D19S226 and D19S902, with a multipoint location score of 2.9 (Figure 2A and Figure S1 available online). Three genes encoding COX structural subunits are contained within this region: the ubiquitously expressed *COX6B1* and *COX7A1* and the testis-specific *COX6B2* isoform. We found no change in *COX7A1* and *COX6B2* genes, but both probands carried a homozygous c.221G→A substitution in exon 2 of *COX6B1*, predicting a p.R19H amino acid change (numeration according to the mature protein in which the first M is eliminated). A pathogenic role for this mutation was suggested by its segregation with the disease according to a recessive trait, its absence in 100 Arab and 1000 Italian control alleles, and the absolute evolutionary conservation

Figure 2.   Genetic, Clinical, and Biochemical Analysis

(A) Family pedigree and haplotype analysis of the *COX6B1* locus. Patients (#15, patient AK; #16, patient AW) are indicated by black symbols.

(B) COX histoenzymatic staining of muscle biopsy. The reaction is diffusely low in the muscle from patient AW, compared with an age-matched control (inset).

(C) Electropherogram of the c.221G→A mutation in exon 2 of the *COX6B1* gene. The alignment of the protein sequence in different species is shown below. The numeration of the amino acid residues corresponds to the mature COX6B1 as the first M is cleaved in the import process of the precursor into mitochondria. The R19 residue and the conserved RFP motif are shown in red and yellow, respectively.

Table 1. Respiratory-Chain-Complex Activities

Tissue and Patient	CI/CS	CII/CS	CIII/CS	CIV/CS	CV/CS	CS[a]
Muscle						
AK	17.8	24.3	136	*37*	238	155
AW	22.7	17.7	131	*26*	234	198
Normal	13.6–27.7	15–28	88–167	120–220	130–280	80–210
Fibroblasts						
AK	29.2	15.3	107	*52*	117	119
AW	33.6	15.3	107	*48*	123	148
Normal	10.7–26	8.6–18.4	86–130	70–125	65–113	100–200

COX/CS values in the patients are in bold italic.
[a] CS, citrate synthase. Activity is expressed as nM/min/mg protein.

Table 2. Cytochrome C Oxidase Activity, Normalized by Citrate Synthase Activity in Control and Patient Immortalized Fibroblasts

Sample	COX/CS[a]
Control.pBabe	100 ± 19 (n = 7)
A.K. pBabe	44 ± 11[b] (n = 9)
A.W. pBabe	50 ± 19[b] (n = 6)

[a] Expressed as % mean control value ± standard deviation (SD).
[b] Student's t test with respect to Control.pBabe: p < 0.0001.

of the R19 residue. The latter is part of a triplet R-F-P motif, which has remained thoroughly invariant from yeast to humans (Figure 2C).

Protein Modeling

Considering the crystal structure of bovine COX, the R19 residue is predicted to form a strong saline bond with the adjacent highly conserved D17 residue and a weaker saline bond with conserved D35 residue. These bonds help maintain the appropriate conformation of the COX6B1 N-terminal loop, which is predicted to interact with subunit 2 of COX (Figure 2D). The substitution of an elongated, flexible R with a bulkier, shorter and rigid H residue may well prevent the formation of the salt bridge with D35, and weaken the salt bridge with D17, as well; this altered conformation could in turn compromise the stability of the COX6B1 subunit within the COX dimer, which is the physiologically active form of the enzyme.

COX6B1 Knockdown Affects Human COX Activity

To investigate the role of the COX6B1 subunit on COX function in a human system, we performed RNA interference assays in HeLa cells. We used COX6B1sh1 and COX6B1sh14, two shRNAs corresponding to specific 3′ UTR sequences of the human *COX6B1* transcript. A real-time quantitative PCR assay showed that COX6B1 mRNA levels were decreased to 40% in both shRNA1 and shRNA14 stably expressing cells compared to mock-transfected cells (Figure 3A). Western-blot analysis showed that COX6B1 protein levels were reduced to approximately 60% of controls (Figure 3C). Accordingly, the COX/CS activities were significantly reduced, to around 70%, in either shRNA1- or shRNA14-versus mock-transfected HeLa cells (p < 0.0026 and p < 0.0009 respectively, Figure 3B). Therefore, reduced incorporation of COX6B1 determines the formation of a functionally impaired enzyme.

Cytochrome C Oxidase Assembly in Patient Tissues

To test as whether the p.R19H mutation could affect the stability of COX, we carried out WB analysis with antibodies specific to several COX subunits. In experiments based on denaturing, sodium dodecyl sulfate-polyacrylamide gel electrophoresis (SDS-PAGE) on mutant versus control muscle homogenate samples, we detected reduced crossreacting material (CRM) for all tested COX subunits, including COX6B1 (Figure 4A). To further investigate the structural composition of mutant COX, we analyzed the holocomplex from muscle homogenates extracted in native conditions and separated by BNGE. As shown in Figure 4A, fully assembled COX was reduced to approximately 40% in mutant versus control muscle. Taken together, these results indicate that the p.R19H change in COX6B1 compromises the stability of the muscle COX holocomplex, thus reflecting the severely reduced specific activity measured in this tissue.

To test whether, and to what extent, the mutant COX6B1[R19H] protein was incorporated into the holocomplex, we carried out BNGE-WB analysis in mitochondria isolated from immortalized fibroblasts, with antibodies against several COX subunits. Incorporated MTCO1, COX4, and COX5A CRMs were present in comparable amounts in mutant versus control fibroblast mitochondria, whereas the amount of mutant COX6B1[R19H] was substantially lower than that of COX6B1[wild-type] (Figure 4B). In addition, the electrophoretic mobility of the COX holocomplex was consistently altered in the mutant samples (Figure 4B). When the same experiment was carried out in denaturing conditions by SDS-PAGE WB analysis, we detected no difference in the amount of any COX-specific CRM, including that corresponding to COX6B1, between mutant and control fibroblast mitochondria. Taken together, these results suggest that mutant COX6B1[R19H] was normally expressed in fibroblasts, but failed to be, or to remain, stably incorporated in the COX holocomplex. The functional relevance of the different electrophoretic mobility of mutant COX holocomplex is unclear, but it may suggest an altered conformation of its quaternary structure.

(D) Modeling of the bovine COX dimer. The COX6B1 and MT-CO2 subunits are in red/blue and yellow, respectively. The mutant R19 residue and the adjacent D17 and D35 residues are also indicated. Relevant nitrogen atoms in R19 and oxygen atoms in D17 and D35 are shown in blue and red, respectively (see main text for details).
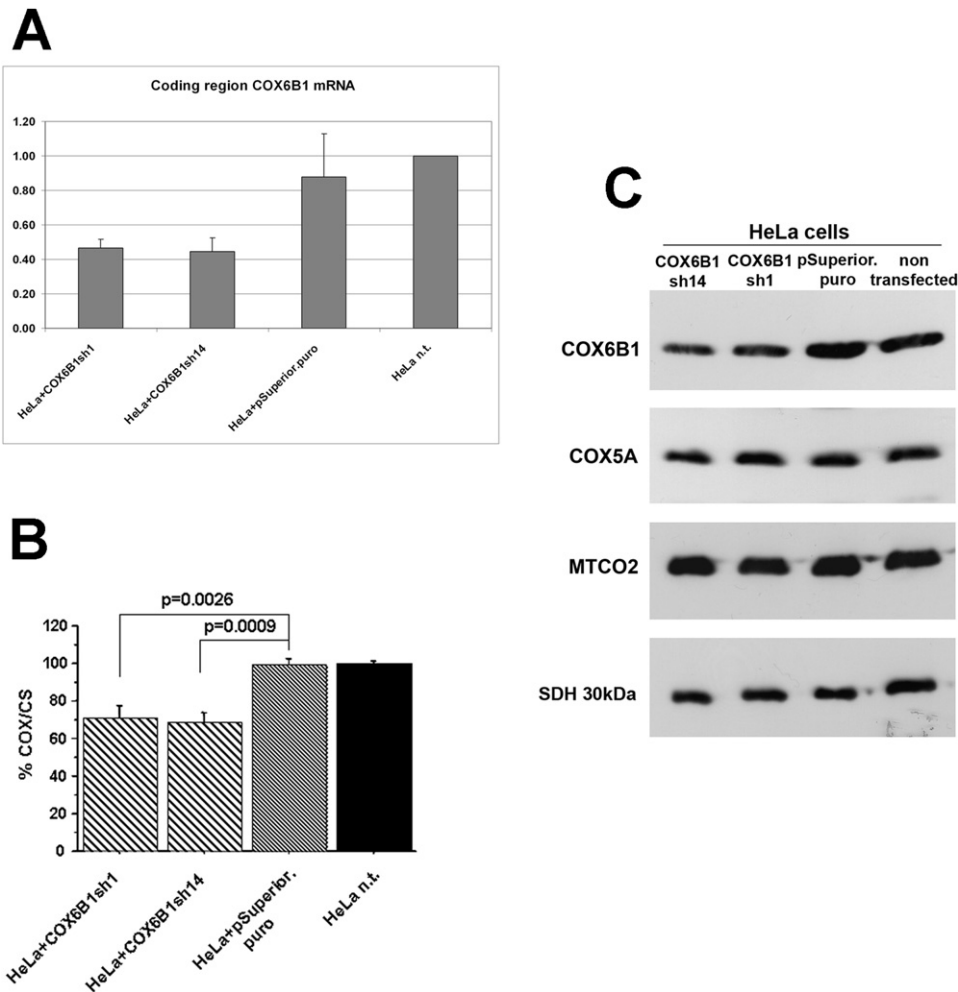
Figure 3. RNA Interference Assays in HeLa Cells

(A) Quantification by RT-PCR of the COX6B1 mRNA levels in the HeLa cells stable expression of the shRNAs corresponding to the sequences number 1 and number 14 with respect to the mock-transfected cells (pSuper.puro) and the nontransfected HeLa cells.

(B) COX/CS activity measured in the HeLa cells stable expression of the shRNAs corresponding to sequences number 1 and number 14 with respect to the mock-transfected cells (pSuper.puro) and the nontransfected HeLa cells. The plotted values are expressed as the percentage of the mean value obtained for the nontransfected HeLa cells $\pm$ SD (n = 3).

(C) Western-blot analysis to determine the protein levels of the COX6B1 subunit and other COX subunits. The antibody against the SDH 30 kDa subunit (complex II) was used for normalization purposes.

Complementation Studies in Yeast
Saccharomyces cerevisiae

In order to validate the pathogenic role of the human $COX6B1^{R19H}$ mutant protein, we first performed complementation studies in BY4741$\Delta cox12$, a *Saccharomyces cerevisiae* strain carrying a deletion of *COX12*, the yeast *COX6B1* gene ortholog. The $\Delta cox12$ strain does not respire and fails to grow in obligatory aerobic media such as those containing 2% ethanol (EtOH) as the only carbon source[26] (see Figure 5A, pYEX strain). The $\Delta cox12$ strain was transformed with either human $COX6B1^{wild-type}$ or mutant human $COX6B1^{R219H}$ cDNAs. EtOH-dependent OXPHOS growth of the $\Delta cox12$ strain was 35% slower, and oxygen consumption was 25% lower in $COX6B1^{R19H}$ than in $COX6B1^{wild-type}$ transformants (Figure 5A and Table 3). Likewise, the activity of COX/CS in $COX6B1^{R19H}$ trans-

formants was 67% to that of the $COX6B1^{wild-type}$ transformants (Figure 5A and Table 3).

Complementation Studies in Human Cells

Transient or stable expression of recombinant $COX6B1^{wild-type}$ and $COX6B1^{R19H}$ cDNAs in HeLa cells failed to modify the COX activity relative to naive or mock-transfected cells, thus excluding that expression of either recombinant construct could per se perturb the function of the enzyme (Figure S2).

To establish the pathogenic role of the R19H mutation in a human in vivo system, we stably expressed $COX6B1^{wild-type}$ and $COX6B1^{R19H}$ cDNAs in immortalized fibroblasts derived from both patients. The stable expression of recombinant $COX6B1^{wild-type}$ was approximately 3-fold that of naive cells, whereas the stable expression of
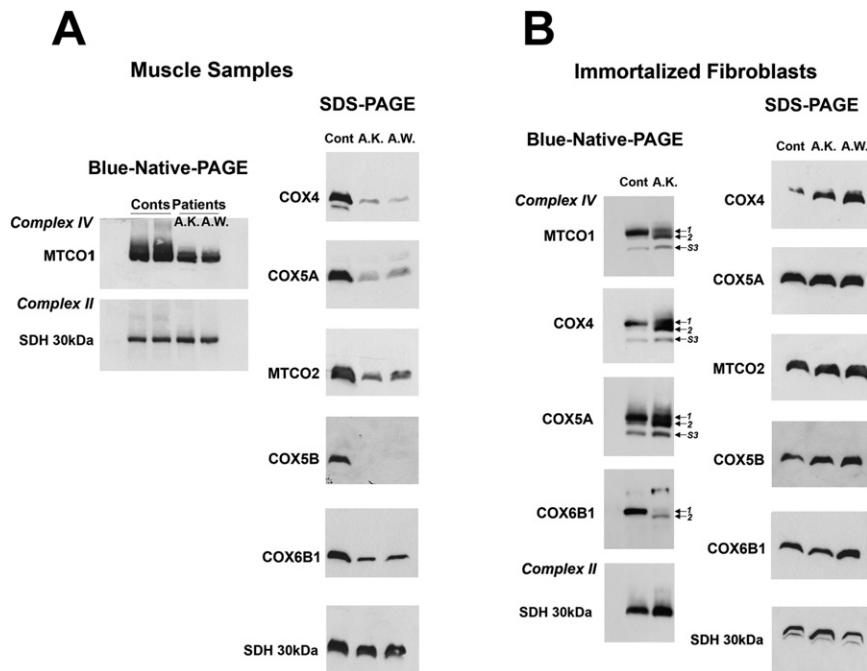
A
Muscle Samples

Blue-Native-PAGE

Conts Patients
A.K. A.W.

Complex IV
MTCO1

Complex II
SDH 30kDa

SDS-PAGE

Cont A.K. A.W.

COX4

COX5A

MTCO2

COX5B

COX6B1

SDH 30kDa

B
Immortalized Fibroblasts

Blue-Native-PAGE

Cont A.K.

Complex IV
MTCO1

COX4

COX5A

COX6B1

Complex II
SDH 30kDa

SDS-PAGE

Cont A.K. A.W.

COX4

COX5A

MTCO2

COX5B

COX6B1

SDH 30kDa

Figure 4. Western-Blot Analysis of COX Subunits
(A) Muscle homogenates. An antibody against the SDH 30 kDa subunit (complex II) was used for normalization. Assembled complex IV holocomplex and individual COX subunits are both decreased.
(B) Mitochondrial fractions from immortalized fibroblasts (see text for details). Arrows 1 and 2 indicate the band doublet corresponding to assembled COX species. S3 corresponds to a COX assembly intermediate.[29–31]

$COX6B1^{R19H}$ was 5- to 6-fold, as confirmed by RFLP densitometry and real-time PCR analysis (Figure S3). Cytochemical staining suggested the recovery of COX-specific reaction in $COX6B1^{wild-type}$-transfected mutant cells (Figure 5B). Accordingly, biochemical analysis showed a 50% increase of COX activity in $COX6B1^{wild-type}$-transfected cells, relative to mock-transfected cells, $p < 0.0001$ (Figure 5C), whereas it remained unchanged in cells transfected with mutant $COX6B1^{R19H}$. In addition, BNGE-WB analysis showed the appearance of a substantial amount of normally migrating COX holocomplex in $COX6B1^{wild-type}$-transfected mutant cells (Figure 5D). Taken together, these results demonstrate that the p.R19H change is associated with the functional and structural COX defect found in our patients.

Discussion

We report here for the first time that a mutation in a nuclear encoded COX subunit (COX6B1) causes a mitochondrial encephalomyopathy due to complex IV deficiency. In addition to the genetic segregation of the mutant allele, the absolute conservation of the R19 aminoacid residue, and the in silico prediction of the structural consequences of the R19H change, several functional data are consistent with this mutation to be deleterious and highlight the role of the COX6B subunit for the enzymatic activity of COX. First, specific reduction of *COX6B* expression determines a parallel reduction of COX activity in HeLa cells. Accordingly, the genetic ablation of Cox12 in yeast leads to severely defective respiration and aerobic growth and marked reduction of the enzyme turnover, although no apparent effect on activity[26] results by detergent-based removal of Cox12 from the holoenzyme. Second, rescue

of the COX defect was obtained in mutant cell lines expressing the recombinant wild-type protein ($COX6B1^{wild-type}$), whereas the defect was not corrected by expressing the mutant species ($COX6B1^{R19H}$). Third, the $\Delta COX12$ yeast strain transformed with the mutant human *COX6B1* ($hcox6b1^{R19H}$) showed a significantly lower growth rate, COX/CS, and respiration activities, compared to the $\Delta COX12$ strain expressing $hcox6b1^{wild-type}$. Fourth, SDS-PAGE and BNGE-WB analyses demonstrated that mutant $COX6B1^{R19H}$ failed to be or remain incorporated in the COX holoenzyme. As a consequence, we observed a reduction of fully assembled COX in muscle and the presence of an aberrant COX-related band in fibroblasts (band 2 in Figures 4B and 5D), possibly due to altered quaternary structure of the mutant enzyme. A faster migrating COX species was also reported in Barth's syndrome, a condition characterized by altered cardiolipin composition of the mitochondrial inner membrane.[27] Interestingly, cardiolipin is involved in the interaction of COX6B1 with the COX holocomplex.[28] Finally, our BNGE-WB analyses clearly show that the S3 COX assembly intermediate, also named subcomplex b,[29,30] of control samples did not contain COX6B1, which was present in the fully assembled COX holocomplex (S4) (see Figure 4B). This result suggests that, contrary to the current view,[31] COX6B1 is incorporated in the very last step of COX assembly.

So far, only mutations of mtDNA encoded COX subunits or nucleus encoded COX assembly factors have been associated with human COX deficiency,[6,7,32] raising the conjecture that mutations in nucleus encoded COX structural subunits were not viable extra utero. However, very recently, mutations that disrupt COX subunit 6A and knockdown of subunit COX5A were reported in *Drosophila*[33] and zebrafish,[34] respectively. Both models do not result in embryonic lethality but rather in neurodegeneration and COX deficiency. In agreement with these experimental models, our own data show that disease-causing abnormalities of nuclear COX subunits are also possible in humans.
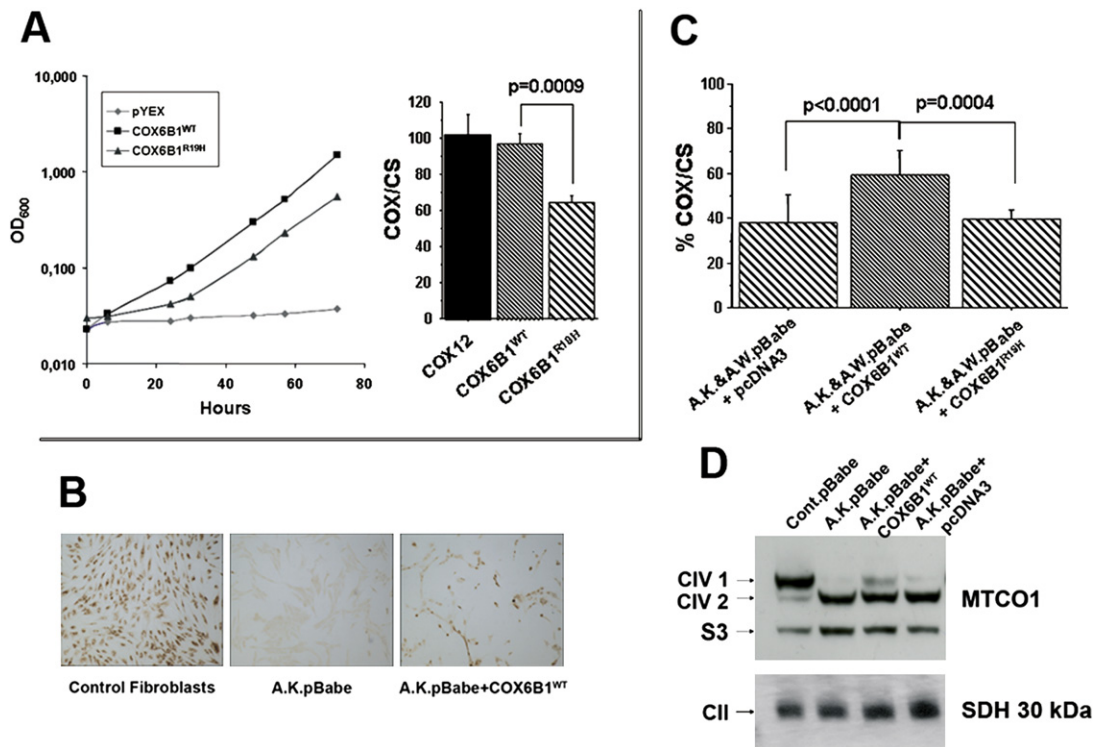
Figure 5. Complementation Studies

(A) Growth of *S. cerevisiae* recombinant ΔCOX12 strains on 2% ethanol-YNB medium transfected with COX6B1[R20H] cDNA, COX6B1[wild-type] cDNA, and the empty pYEX expression vector.

(B) Cytochemical reaction to COX in fibroblast cell lines.

(C) COX/CS activities, expressed as percentage of the mean control value ± SD, in immortalized fibroblasts and recombinant derivatives, transfected as indicated (A.K. & A.W. pBabe + pcDNA3: n = 13; A.K. & A.W. pBabe + *COX6B1[wild-type]*: n = 15; A.K. & A.W. pBabe + *COX6B1[R19H]*: n = 6).

(D) BNGE-WB analysis of COX in transfected cells. Gel gradient was 7%–10% for better separation of the COX holocomplex doublet (CIV 1 and CIV 2).

Supplemental Data

Three figures are available at http://www.ajhg.org/.

Table 3. Effect of Mutations on Respiration in Haploid BY4741 Δcox12 Strain

Allele[a]	Respiration[b]	COX/CS[d]
No allele	<2	<1
COX12	42 ± 4	100 ± 11
COX6B1[wild-type]	29 ± 2[c]	97 ± 5
COX6B1[R19H]	19 ± 3[c]	65 ± 3

[a] Allele carried by the vector introduced into the strain.

[b] Expressed as µl O2/h/mg dry weight. Each value is the mean ± SD of three independent experiments.

[c] Student's t test for Respiration: *COX6B1[wild-type]* versus *COX6B1[R19H]* p < 0.007.

[d] Student's t test for COX/CS values: *COX6B1[wild-type]* versus *COX6B1[R19H]* p < 0.0009; *COX12* versus *COX6B1[R19H]* p < 0.005; *COX12* versus *COX6B1[wild-type]* p = 0.5.

Web Resources

The URLs for data presented herein are as follows:

Online Mendelian Inheritance in Man (OMIM), http://www.ncbi.nlm.nih.gov/Omim/

Protein Interaction Calculator, http://crick.mbu.iisc.ernet.in/~PIC/index.html

RNA interference target calculation, http://www.genscript.com

References

1. Grossman, L.I., and Lomax, M.I. (1997). Nuclear genes for cytochrome c oxidase. Biochim. Biophys. Acta *1352*, 174–192.

2. Tsukihara, T., Aoyama, H., Yamashita, E., Tomizaki, T., Yamaguchi, H., Shinzawa-Itoh, K., Nakashima, R., Yaono, R., and Yoshikawa, S. (1996). The whole structure of the 13-subunit oxidized cytochrome c oxidase at 2.8 A. Science *272*, 1136–1144.

3. Yoshikawa, S., Shinzawa-Itoh, K., and Tsukihara, T. (1998). Crystal structure of bovine heart cytochrome c oxidase at 2.8 A resolution. J. Bioenerg. Biomembr. *30*, 7–14.

4. Sampson, V., and Alleyne, T. (2001). Cytochrome c/cytochrome c oxidase interaction. Direct structural evidence for conformational changes during enzyme turnover. Eur. J. Biochem. *268*, 6534–6544.

5. Hüttemann, M., Jaradat, S., and Grossman, L.I. (2003). Cytochrome c oxidase of mammals contains a testes-specific isoform of subunit VIb–the counterpart to testes-specific cytochrome c? Mol. Reprod. Dev. *66*, 8–16.

6. Barrientos, A., Barros, M.H., Valnot, I., Rotig, A., Rustin, P., and Tzagoloff, A. (2002). Cytochrome oxidase in health and disease. Gene *286*, 53–63.

7. Pecina, P., Houstkova, H., Hansikova, H., Zeman, J., and Houstek, J. (2004). Genetic defects of cytochrome c oxidase assembly. Physiol. Res. *53 (Suppl 1)*, S213–S223.

8. DiMauro, S., and De Vivo, D.C. (1996). Genetic heterogeneity in Leigh syndrome. Ann. Neurol. *40*, 5–7.

9. Adams, P.L., Lightowlers, R.N., and Turnbull, D.M. (1997). Molecular analysis of cytochrome c oxidase deficiency in Leigh's syndrome. Ann. Neurol. *41*, 268–270.

10. Jaksch, M., Hofmann, S., Kleinle, S., Liechti-Gallati, S., Pongratz, D.E., Muller-Hocker, J., Jedele, K.B., Meitinger, T., and Gerbitz, K.D. (1998). A systematic mutation screen of 10 nuclear and 25 mitochondrial candidate genes in 21 patients with cytochrome c oxidase (COX) deficiency shows tRNA (Ser)(UCN) mutations in a subgroup with syndromal encephalopathy. J. Med. Genet. *35*, 895–900.

11. Coenen, M.J., Smeitink, J.A., Pots, J.M., van Kaauwen, E., Trijbels, F.J., Hol, F.A., and van den Heuvel, L.P. (2006). Sequence analysis of the structural nuclear encoded subunits and assembly genes of cytochrome c oxidase in a cohort of 10 isolated complex IV-deficient patients revealed five mutations. J. Child Neurol. *21*, 508–511.

12. Sobel, E., and Lange, K. (1996). Descent graphs in pedigree analysis: Applications to haplotyping, location scores, and marker-sharing statistics. Am. J. Hum. Genet. *58*, 1323–1337.

13. Sobel, E., Sengul, H., and Weeks, D.E. (2001). Multipoint estimation of identity-by-descent probabilities at arbitrary positions among marker loci on general pedigrees. Hum. Hered. *52*, 121–131.

14. Sobel, E., Papp, J.C., and Lange, K. (2002). Detection and integration of genotyping errors in statistical genetics. Am. J. Hum. Genet. *70*, 496–508.

15. Mukhopadhyay, N., Almasy, L., Schroeder, M., Mulvihill, W.P., and Weeks, D.E. (2005). Mega2: Data-handling for facilitating genetic linkage and association analyses. Bioinformatics *21*, 2556–2557.

16. Tiranti, V., Hoertnagel, K., Carrozzo, R., Galimberti, C., Munaro, M., Granatiero, M., Zelante, L., Gasparini, P., Marzella, R., Rocchi, M., et al. (1998). Mutations of SURF-1 in Leigh disease associated with cytochrome c oxidase deficiency. Am. J. Hum. Genet. *63*, 1609–1621.

17. Bugiani, M., Invernizzi, F., Alberio, S., Briem, E., Lamantea, E., Carrara, F., Moroni, I., Farina, L., Spada, M., Donati, M.A., et al. (2004). Clinical and molecular findings in children with complex I deficiency. Biochim. Biophys. Acta *1659*, 136–147.

18. Wharton, D.C., and Tzagoloff, A. (1967). Cytochrome oxidase from beef heart mitochondria. Methods Enzymol. *10*, 245–250.

19. Fernández-Vizarra, E., López-Perez, M.J., and Enríquez, J.A. (2002). Isolation of biogenetically competent mitochondria from mammalian tissues and cultured cells. Methods *26*, 292–297.

20. Bresolin, N., Zeviani, M., Bonilla, E., Miller, R.H., Leech, R.W., Shanske, S., Nakagawa, M., and DiMauro, S. (1985). Fatal infantile cytochrome c oxidase deficiency: Decrease of immunologically detectable enzyme in muscle. Neurology *35*, 802–812.

21. Nijtmans, L.G., Henderson, N.S., and Holt, I.J. (2002). Blue Native electrophoresis to study mitochondrial and other protein complexes. Methods *26*, 327–334.

22. Schägger, H. (1996). Electrophoretic techniques for isolation and quantification of oxidative phosphorylation complexes from human tissues. Methods Enzymol. *264*, 555–566.

23. Gietz, R.D., and Woods, R.A. (2002). Transformation of yeast by lithium acetate/single-stranded carrier DNA/polyethylene glycol method. Methods Enzymol. *350*, 87–96.

24. Sambrook, J., and Russel, D.W. (2001). Molecular Cloning: A Laboratory Manual (Cold Spring Harbor, NY: Cold Spring Harbor Laboratory Press).

25. Ferrero, I., Viola, A.M., and Goffeau, A. (1981). Induction by glucose of an antimycininsensitive, azide-sensitive respiration in the yeast Kluyveromyces lactis. Antonie Van Leeuwenhoek *47*, 11–24.

26. LaMarche, A.E., Abate, M.I., Chan, S.H., and Trumpower, B.L. (1992). Isolation and characterization of COX12, the nuclear gene for a previously unrecognized subunit of Saccharomyces cerevisiae cytochrome c oxidase. J. Biol. Chem. *267*, 22473–22480.

27. McKenzie, M., Lazarou, M., Thorburn, D.R., and Ryan, M.T. (2006). Mitochondrial respiratory chain supercomplexes are destabilized in Barth Syndrome patients. J. Mol. Biol. *361*, 462–469.

28. Sedlak, E., and Robinson, N.C. (1999). Phospholipase A(2) digestion of cardiolipin bound to bovine cytochrome c oxidase alters both activity and quaternary structure. Biochemistry *38*, 14966–14972.

29. Williams, S.L., Valnot, I., Rustin, P., and Taanman, J.W. (2004). Cytochrome c oxidase subassemblies in fibroblast cultures from patients carrying mutations in COX10, SCO1, or SURF1. J. Biol. Chem. *279*, 7462–7469.

30. Stiburek, L., Vesela, K., Hansikova, H., Pecina, P., Tesarova, M., Cerna, L., Houstek, J., and Zeman, J. (2005). Tissue-specific cytochrome c oxidase assembly defects due to mutations in SCO2 and SURF1. Biochem. J. *392*, 625–632.

31. Nijtmans, L.G., Taanman, J.W., Muijsers, A.O., Speijer, D., and Van den Bogert, C. (1998). Assembly of cytochrome-c oxidase in cultured human cells. Eur. J. Biochem. *254*, 389–394.

32. Zeviani, M., and Di Donato, S. (2004). Mitochondrial disorders. Brain *127*, 2153–2172.

33. Liu, W., Gnanasambandam, R., Benjamin, J., Kaur, G., Getman, P.B., Siegel, A.J., Shortridge, R.D., and Singh, S. (2007). Mutations in cytochrome c oxidase subunit VIa cause neurodegeneration and motor dysfunction in Drosophila. Genetics *176*, 937–946.

34. Baden, K.N., Murray, J., Capaldi, R.A., and Guillemin, K. (2007). Early developmental pathology due to cytochrome c oxidase deficiency is revealed by a new zebrafish model. J. Biol. Chem. *282*, 34839–34849.